Photochemical & Photobiological Sciences (2025) 24:991–1002
https://doi.org/10.1007/s43630-025-00740-9

ORIGINAL PAPERS

Enhanced UV-C resistance through light-activated zinc-cysteine complex formation

Martin Fuleky[1] · Katarina Molnarova[1] · Jan Novak[2] · Milada Vodova[1] · Libor Lenza[1] · Lukas Nejdl[1,3]

Received: 21 February 2025 / Accepted: 12 May 2025 / Published online: 25 May 2025

Abstract

Ultraviolet (UV) radiation is a significant environmental stressor that affects the growth, physiology, and biochemical integrity of various organisms. This study investigates the potential protective effects of a zinc-cysteine (Zn–Cys) complex against UV-C radiation, with a focus on its impact on selected microalgae (*Coccomyxa peltigera*e and *Parachlorella kessleri*) and maize (*Zea mays L.*). We demonstrate that exposure of the Zn–Cys complex to UV-C (254 nm) results in the formation of fluorescent photoproducts, which exhibit UV-protective properties. The study reveals that Zn–Cys significantly mitigates UV-induced stress. In both microalgae species, the Zn–Cys complex enhanced growth even under UV exposure, with the 20% concentration showing the most robust protective effects. Further hyperspectral imaging confirmed the protective mechanism of Zn-Cys by monitoring changes in light reflectance in *Parachlorella kessleri*, indicating reduced photosynthetic efficiency and structural alterations induced by UV exposure, while Zn–Cys significantly mitigated these effects. In addition, in maize plants (*Zea mays L.*), Zn–Cys treatment preserved chlorophyll content and reduced polyphenol accumulation, indicating reduced oxidative stress. These findings highlight the potential of the Zn–Cys complex as a sustainable and cost-effective strategy for UV protection in both terrestrial and extraterrestrial agriculture, advancing our understanding of plant adaptation to extreme environments.

Keywords Hyperspectral imaging · Microalgae · Plants · Spectrophotometry · UV protection

1 Introduction

Light-driven reactions represent a pivotal area of modern science and technology with wide-ranging applications across various fields [1–3]. For example, photochemical reactions of thiol-ene, commonly known as thiol-ene click reactions, are a class of highly efficient, versatile chemical processes that involve the photoinitiated addition of a thiol group (–SH) to an alkene (C=C) via a radical mechanism [4].

In our recent work, we demonstrated that light-driven reactions involving thiol groups (–SH) in combination with metal ions (Cu^{2+}, Zn^{2+}, Cd^{2+}, Se^{4+}) lead to the synthesis of nanoparticles, including fluorescent zinc-cadmium quantum dots (ZnCd QDs [5, 6]), copper nanoparticles, and selenium nanoparticles [7].

Based on this work, we hypothesize that the properties of these light-driven reactions can be leveraged to explore their UV-protective mechanisms. Developing efficient, cost-effective, and sustainable strategies to protect plants from harmful UV radiation remains a major area of interest, with a focus on significantly increasing plant production efficiency [8, 9]. Moreover, leveraging harmful UV radiation for beneficial purposes carries profound implications for space technologies, particularly in the context of planetary colonization, such as on Mars, where UV radiation poses a significant challenge [10]. The development of protective mechanisms that exploit UV radiation could, therefore, provide transformative benefits for agricultural

✉ Lukas Nejdl
lukasnejdl@gmail.com

[1] Department of Chemistry and Biochemistry, Mendel University in Brno, Zemědělská 1665/1, 613 00 Brno, Czech Republic

[2] Department of Molecular Biology and Radiobiology, Mendel University in Brno, Zemědělská 1665/1, 613 00 Brno, Czech Republic

[3] J. Heyrovsky Institute of Physical Chemistry, Czech Academy of Sciences, Dolejškova 3, 182 23 Prague, Czech Republic

and ecological applications in both terrestrial and extraterrestrial environments.

Taking these factors into account, we investigated the potential protective effects of the L-cysteine and zinc acetate complex (Zn–Cys) against UV-C radiation. The Zn–Cys complex forms spontaneously under mild laboratory conditions (25 °C and atmospheric pressure) from its precursors [11] and, as we demonstrate in this study, produces newly fluorescent Zn/Cys photoproducts upon UV-C exposure. The phototransformation of the Zn–Cys complex by UV-C, along with its resulting photoproducts, exhibits a protective effect against UV-C radiation.

As the experimental model for evaluating the protective effects of the Zn–Cys complex against UV-C radiation, as well as its toxicity both prior to and following UV exposure, we have chosen microalgae (*Coccomyxa peltigerae* and *Parachlorella kessleri*) and maize plants (*Zea mays L.*) cultured under in vitro conditions. Microalgae are recognized for their potential as biofertilizers and soil conditioning agents, enhancing soil fertility and promoting plant productivity [12–14]. Algal-based fertilizers are easy to use and cost-effective, increasing soil's moisture retention capacity, humus formation, and nutrient uptake, among other benefits [15, 16]. In addition, microalgae serve as valuable tools for assessing the toxicity of various substances due to their rapid growth and sensitivity to environmental changes and pollutants. They can provide quick and reliable indicators of toxicity, helping researchers understand the potential effects of different substances on phototrophic organisms and entire ecosystems [17–19]. Similarly, maize is a vital crop known for its high productivity. As a major source of food and biofuel, maize plays an essential role in agricultural systems [20, 21]. The combination of microalgae and maize in our experimental model allows for a comprehensive assessment of the protective effects of the Zn–Cys complex on both aquatic and terrestrial systems.

The exploration of such protective mechanisms may offer new avenues for both terrestrial and extraterrestrial agriculture, ensuring plant survival and growth in extreme environments.

2 Materials and methods

2.1 Chemicals

The following chemicals were used: sodium phosphate monobasic monohydrate (Sigma–Aldrich, ≥ 98.00%), sodium phosphate dibasic (Sigma–Aldrich, 99.00%), zinc acetate (Sigma–Aldrich 99.99%), L-cysteine (Sigma–Aldrich 97.00%), TWEEN® 20 (Sigma–Aldrich), TAP medium, MS medium (Duchefa), Sucrose (99.5%, Sigma–Aldrich), agar (Duchefa), hypochlorite, ethanol, and ddH_2O.

2.2 Preparation of zinc and cysteine precursors and their complex (Zn-Cys)

For the preparation of Zn and Cys precursor stocks, 30 mM zinc acetate (Zn^{2+}), 50 mM L-cysteine (Cys), and 100 mM phosphate buffer (pH 7) were used. The phosphate buffer was prepared by mixing sodium phosphate monobasic monohydrate and sodium phosphate dibasic and adjusting the pH to 7. To prepare 100 mL of Zn–Cys complex mixture, 50 mL of phosphate buffer pH 7, 12.5 ml of Cys, 12.5 ml of ddH_2O, and 25 ml of Zn^{2+} were mixed. The Zn–Cys complex forms spontaneously under mild laboratory conditions (25 °C and atmospheric pressure) from its precursors [11].

To evaluate the protective effect of the Zn–Cys complex against UV-C radiation, several experimental conditions were designed in which either the Zn–Cys complex or its photoproducts (Zn/Cys) were introduced into a biological system. In the first condition, the Zn–Cys complex was added without subsequent UV irradiation (marked Zn–Cys). In the second condition, the Zn–Cys complex was introduced into the biological system, which was then exposed to UV-C radiation for 10 min; this setup is referred to as Zn–Cys + UV. In the third condition, preformed Zn/Cys photoproducts—generated by exposing the Zn–Cys complex to UV-C for 30 min—were added to the system. If this system was subsequently subjected to UV-C irradiation for 10 min, the condition is denoted as Zn/Cys + UV.

2.3 UV irradiation of Zn-Cys complex and spectral characterization

The Zn-Cys complex (Zn^{2+} and Cys in phosphate buffer, pH 7) was transferred in triplicate into a UV-transparent, flat-bottomed 96-well plate (Costar, Corning, USA), with each well containing 100 µL. Samples were irradiated for 0, 10, and 30 min using a UV transilluminator (Vilber Lourmat, Marne-la-Vallée Cedex, France) emitting light at 254 nm. For Zn/Cys photoproducts creation, the Zn–Cys complex was irradiated with UV-C light for 30 min prior to experiments. The illumination area, measuring 20 × 20 cm, was exposed to six emitting tubes, each rated at 25 W. The intensity of the UV radiation incident on the sample was measured with an optical power meter (PM100D, sensor SV120VC, Thorlabs Inc., Newton, NJ, USA), yielding an intensity of $E = 0.40$ mW/mm^2.

Fluorescence characterization of all samples was performed using the same UV-transparent, flat-bottomed 96-well plate across the spectral range of 250–600 nm with a resolution of 10 nm. Measurements were conducted at

a standard laboratory temperature of 25 °C using a multifunctional modular plate reader Synergy H1 instrument (Biotek, USA). The resulting fluorescence data were processed to generate Excitation-Emission Maps (EEMs) using OriginPro software for advanced data analysis and visualization.

2.4 Screening of toxicity and UV protective properties of Zn and Cys using microalgae

For the first experiment, *Coccomyxa peltigerae* was used due to its susceptibility to UV light and changes to its environmental conditions (Molnarova et al., unpublished). We tested toxic effects and UV protective properties of zinc acetate, L-cysteine, Zn–Cys and Zn/Cys photoproducts. The UV protective properties and toxicity of the Zn–Cys complex were further evaluated using varying concentrations of its precursors in the cultivation media (Table 1). Fresh cells in the exponential growth phase were inoculated into sterile Tris–Acetate-Phosphate (TAP) medium (pH 7) with or without the presence of tested substances and irradiated with UV-C light (254 nm) with intensity of 1 J/cm^2/s for 10 min using UVP Crosslinker CX-2000 (Analytik Jena, Germany). The cultures were then maintained at 23 °C, illuminated with 100 µmol/m^2/s^1 PAR (with 12 h/12 h light/dark regime) using an orbital shaker for the duration of the experiment (96 h). Throughout this period, optical density (Absorbance at 750 nm) was monitored using an Infinite M200 Pro (Tecan, Männedorf, Switzerland) with Tecan i-control software, and the results were expressed as OD750 values against blank.

For a second experiment, we used *Parachlorella kessleri* for its higher tolerance to UV radiation and abiotic stressors [22, 23]. We tested the most promising concentration of Zn–Cys in a media (20%) based on results from the first experiment. The methodology of the experiment and cultivation was the same as that of *C. peltigerae* but results were evaluated for 168 h. For all experiments with microalgae, pH of medium (control and treatment) was 7.

2.5 Hyperspectral imaging

Hyperspectral imaging of microalgae was conducted using a Specim IQ hyperspectral camera (Specim, Finland) with halogen light bulbs serving as the illumination source. Algae samples (*P. kessleri*) were imaged with a white reference Teflon tile (Specim, Finland) for reflectance normalization. Data analysis was carried out using MATLAB software. In accordance with previous recommendations [24], the final spectral band was excluded from the analysis. Each spectral band was filtered using a 3 × 3 Gaussian convolution kernel. Regions of interest (ROIs) were manually selected, and the data represent the average of three biologically independent cultivations. Principal component analysis (PCA) was performed in MATLAB, with the visualized results accounting for over 98% of the total data variability.

Table 1 Calculated concentrations of Zinc (Zn^{2+}) and cysteine (Cys) in different Zn–Cys solutions

Solution	Zn^{2+} concentration	Cys concentration
20%	0.534 mM	1.250 mM
10%	0.267 mM	0.625 mM
5%	0.134 mM	0.3125 mM

2.6 Plant experiment

Hybrid F1 maize seeds of the variety 'Andrea' (SEMO, Smržice, Czech Republic), were utilized for all experiments. Initially, the maize seeds were soaked in 80% ethanol for 5 min while being stirred continuously. After the ethanol was drained, the seeds were incubated in a 5% hypochlorite solution containing TWEEN® 20 detergent (Sigma, France) for 40–50 min with ongoing stirring. Following this, the seeds went through five wash cycles with sterile double-distilled water (ddH2O) and were soaked overnight in sterile ddH_2O. Finally, the seeds were rinsed with a 2.5% hypochlorite solution that included TWEEN® 20 detergent (Sigma, France) and underwent another five wash cycles with sterile ddH2O to ensure the complete removal of hypochlorite.

Sterilized maize seeds were placed in Petri dishes containing ½ MS medium, which comprised 0.22 g of Murashige and Skoog including vitamins (Duchefa Biochem, The Netherlands), 3 g of sucrose (Serva Electrophoresis GmbH, Germany), and 0.8 g of agar (Duchefa Biochem, The Netherlands), for 100 ml of cultivation medium. The seeds were allowed to germinate for 7 days. After this period, the germinated seeds were transferred to glass bottles filled with ½ MS medium, where they continued to grow for an additional 7 days. Any non-germinated or contaminated seeds were eliminated. The culture conditions were maintained consistently at 23 °C, with a light cycle of 16 h of light and 8 h of darkness, at an intensity of 100 µmol/m^2/s^1. Following the 7-day growth period, the solution of zinc-cysteine precursors (most effective concentration (20%), based on previous experiments, was applied to cover the entire leaf surface, and some plants were irradiated with UV-C light for 20 min. A total of four treatments were evaluated: 1. Control (sprayed with ddH2O); 2. Control + UV; 3. Zinc/cysteine (sprayed with solution of zinc cysteine precursors); 4. Zinc/cysteine + UV. Subsequently, every 2 days, the UV-labeled variants received additional UV-C irradiation for 20 min, totaling four irradiations. The entire experiment lasted 15 days. The day following the final irradiation, the aerial parts of the plants were harvested, immediately frozen

in liquid nitrogen, and then lyophilized for 4 days using a FreeZone 2.5 L (Labconco, Kansas City, U.S.). Each variant contained three glass bottles and glass bottle contained three maize plants, resulting in mixed samples. These samples were subsequently cut, homogenized into a coarse powder, and stored at −20 °C for future analysis.

2.7 Spectrophotometric analyses

2.7.1 Total chlorophyll A and B content

Lyophilized samples (approximately 10 mg) were homogenized in 1 ml of 96% ethanol using the Precellys Evolution Homogenizer (Bertin-Instruments, France). This process involved four cycles of 30 s each, with 30 s pauses in between, operating at 6800 rpm. The total concentrations of chlorophyll A and B were determined by measuring absorbance in ethanol at wavelengths of 470, 649, and 665 nm, following the methodology outlined by Lichtenthaler et al. [25].

2.7.2 Total polyphenol content

Approximately 10 mg of lyophilized samples were homogenized using the Precellys Evolution homogenizer (Bertin-Instruments, France) at 6800 rpm for four 30 s cycles, with 30 s intervals between each cycle, in 1 ml of 80% methanol. Following homogenization, the samples were incubated at 60 °C for 2 h. Polyphenol content was then quantified by measuring absorbance at 760 nm using the Folin–Ciocalteu reagent through spectrophotometric analysis [26].

2.7.3 Total protein content

Approximately 10 mg of lyophilized samples were homogenized in 250 µl of protein extraction buffer (comprising 50 mM phosphate buffer, 1 mM EDTA, polyvinyl polypyrrolidone, and protease inhibitor) using a Precellys Evolution homogenizer (Bertin-Instruments, France). The homogenization process was conducted at 6800 rpm for four 30 s cycles, with 30 s pauses between cycles. Total protein concentration was subsequently quantified using a modified Bradford assay, with absorbance measured spectrophotometrically at 595 nm [27].

2.8 Statistical analysis

All treatments and controls were prepared in triplicate biological replicates. For each biological replicate, three technical replicates were measured, resulting in a total of n = 9 data points per treatment. Data processing was conducted using Microsoft Excel (Microsoft Office 365, Microsoft Corporation), while statistical analyses were performed with STATGRAPHICS Centurion XV (Statgraphics Technologies, Inc.). A one-way analysis of variance (one-way ANOVA) was employed to assess the data, with a significance threshold set at $p < 0.05$. Results are presented as the mean ± standard error of the mean and significant differences between groups are denoted by different capital letters on the graphs.

3 Results and discussion

3.1 Fluorescence characterization of Zn-Cys and Zn/Cys photochemistry

The Zn-Cys complex is typically characterized by the coordination of Zn^{2+} with multiple ligands, including the thiol group (–SH), the ammonium group ($–NH_3^+$), and the carboxyl group (–COO–) of cysteine [28, 29]. Zn–Cys complexes often exhibit hexacoordination, meaning that zinc is surrounded by six ligands [28]. Upon binding with zinc, the thiol and ammonium groups of Cys undergo deprotonation, facilitating a strong interaction between Zn and Cys. The resulting structure is stable at physiological pH (~ 7) and plays a critical role in biological systems [11]. When this complex (Zn–Cys) is exposed to UV-C radiation ($\lambda = 254$ nm), the resulting zinc/cysteine (Zn/Cys) photoproduct exhibits intriguing fluorescence properties. Figure 1A shows the emission scan ($\lambda_{ex} = 290$ nm) of the Zn–Cys complex before UV-C exposure (0 min) and the resulting photoproduct Zn/Cys with a λ_{max} of 380 nm after 30 min UV-C treatment. An increase in fluorescence intensity was not observed for the individual precursors of the complex (Cys and Zn) after UV-C treatment. Figure 1B and C illustrates the relationship between fluorescence intensity and the duration of UV-C exposure, ranging from 0 to 30 min, measured using an excitation scan (230–700 nm) with a fixed emission wavelength of 400 nm. A significant formation of Zn/Cys photoproducts was observed between 10 and 30 min of UV-C exposure. However, it is highly likely that their formation begins immediately upon UV treatment. Due to the initially low fluorescence response, their presence could not be detected during the first 10 min of irradiation using fluorescence-based measurements. Nonetheless, the results of the biological experiments (see below) indicate that the Zn–Cys complex exerts a protective effect from the very beginning of UV-C irradiation of the biological system.

As the exposure time increases, the fluorescence intensity also rises, indicating the formation of the photoproduct. Based on the excitation scan (Fig. 1C), it is evident that the resulting photoproduct can be effectively excited within the range of 230–350 nm. This suggests that the generated photoproduct may offer protection against

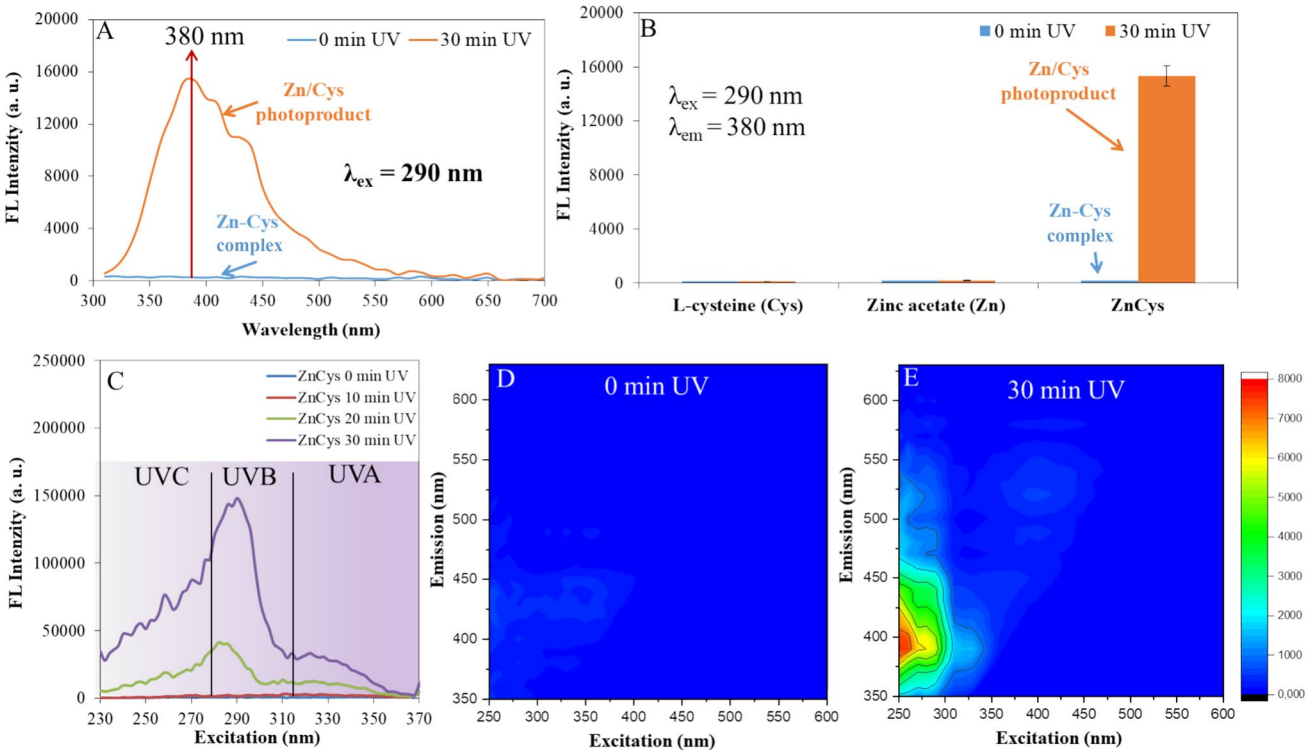

Fig. 1 Effect of UV radiation (254 nm) on the formation of new photoproducts (Zn/Cys) from the Zn–Cys complex. **A** Emission scan in the range of 300–700 nm upon excitation at 290 nm before and after 30 min of UV exposure. **B** The bar graph of the precursors (L-cysteine and zinc acetate) and their combination, showing fluorescence upon excitation at 290 nm and emission at 290 nm before and after 30 min of UV exposure. **C** Excitation scan recorded within the range of 230–370 nm at a fixed emission of 400 nm, measured at time intervals of 0, 10, 20, and 30 min of UV exposure. **D** EEM prior to UV exposure and **E** EEM after 30 min of UV exposure (the fluorescence intensity is represented as a color scale)

radiation, particularly within the 250–350 nm range. This protective effect against UV-C radiation has been confirmed in model organisms, as demonstrated later in this publication. The complete fluorescence characteristics were studied using excitation-emission maps (EEMs), as shown in Fig. 1D (0 min UV) and Fig. 1E (30 min UV). We reported the ability to produce fluorescently active photoproducts during the study of quantum dot QDs synthesis, where a zinc-mercaptosuccinic acid complex exhibited fluorescence with a maximum emission at 402 nm and a quantum yield of 3% after 10 min of UV exposure [30]. The Zn/Cys photoproduct has not yet been adequately characterized; however, based on the obtained results, we hypothesize that nano-sized aggregates (clusters) similar to QDs may form in solution (see more in Sect. 3.1 of the supplementary materials).

Naturally occurring fluorescence has been observed across a wide range of species, from bacteria to birds [31]. In macroscopic animals, such as birds, fluorescence serves as a visual communication signal; however, its functional significance remains largely unknown [32]. While some organisms exhibit photoprotection attributed to fluorescence under UV light, direct experimental evidence is lacking. For instance, Harikumar R. Suma and collective demonstrated that a fluorescent extract from *Paramacrobiotus sp.* can protect the UV-sensitive tardigrade *Hypsibius exemplaris* and the nematode *Caenorhabditis elegans* from germicidal UV radiation [33].

3.2 Toxicity and UV protective properties of zinc and cysteine using C. peltigerae

First, the toxic effect of various concentrations of Cys, Zn, Zn–Cys, and Zn/Cys photoproducts was evaluated on *C. peltigerae,* Fig. 2. In our experiment, Cys (Fig. 2A) and Zn (Fig. 2B) exhibited the highest levels of toxicity towards *C. peltigerae*. In contrast, the Zn–Cys complex (Fig. 2C) and its photoproducts (Fig. 2D) demonstrated a significantly reduced toxic effect, particularly at the highest concentrations tested, when compared to the individual effects of Cys or Zn. At 24 h and 48 h, the Zn–Cys even proved better growth compared to the control, indicating some positive growth effect in the early to middle stages of the experiment. Toxic effect of Zn depends on concentration and on specific demands of different type of microalgae [34]. Concentration of Zn higher than 2.4 mg/l (in the form of ZnO

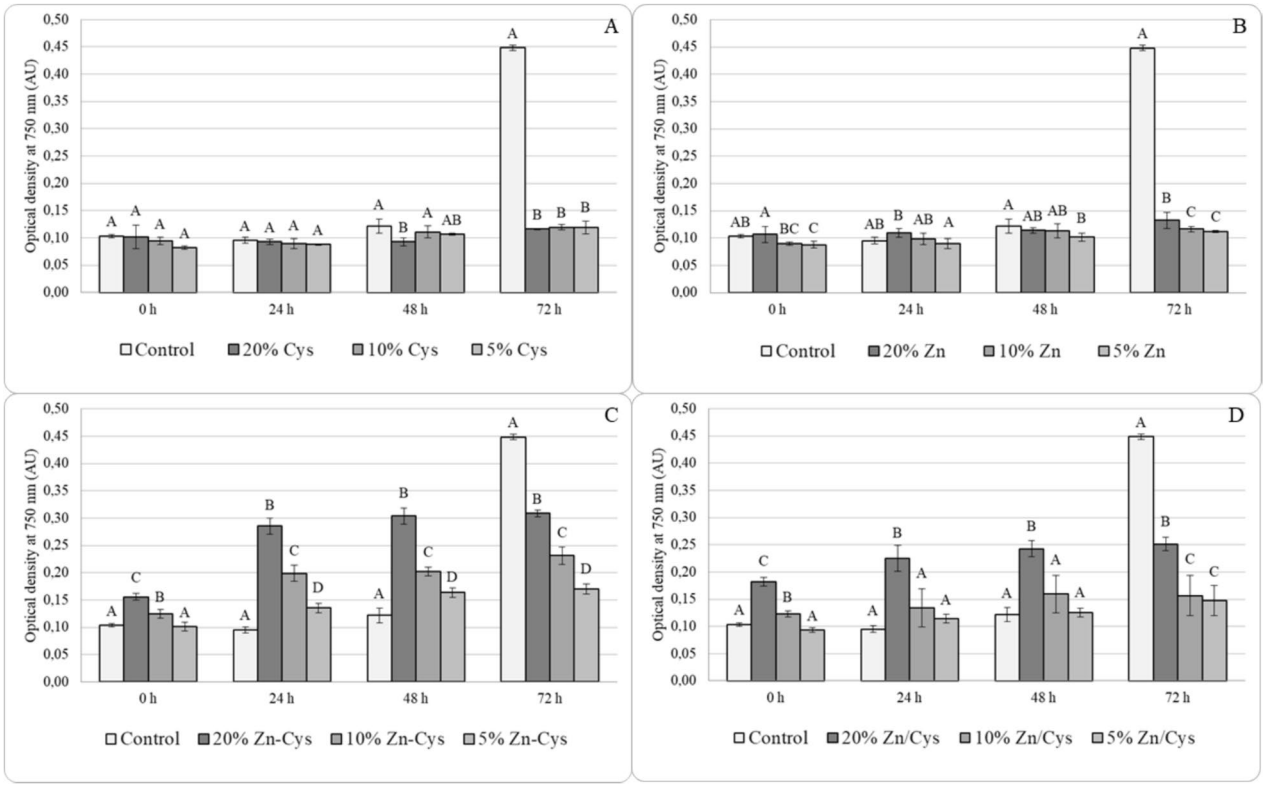

Fig. 2 Growth rate of *C. peltigerae* showing toxic effects of 5, 10, and 20% concentrations: **A** cysteine, **B** zinc acetate, **C** Zn–Cys complex, and **D** Zn/Cys photoproducts. The Zn/Cys photoproduct treatment consisted of a Zn–Cys solution that had been pre-irradiated with UV-C light (254 nm) for 30 min outside of the biological system, prior to its application to algal cultures. The results are expressed as the mean ± standard error of the mean, and significant differences for different days are indicated by different capital letters in the graph (one-way ANOVA). A p value of < 0.05 was considered to indicate a significant difference between groups, $n = 9$

nanoparticles) was proven to be toxic to microalgae *Raphidocelis subcapitata* [35] and our experiment suggests similar effect on *C. peltigerae*. Algae from *Coccomyxa* genus also exhibit high capacity for accumulating metals leading to increased oxidative stress [36]. Cysteine can also be toxic to microalgae through various mechanisms, for example it can alter redox state of cells which contributes to oxidative stress in microalgae [37], or it may disrupt metal detoxification pathway by reducing phytochelatin synthesis [38], which may explain the negative effect of L-cysteine or zinc acetate present in our experiment. In microalgae, Cys contributes to the formation of glutathione and phytochelatins, which bind to metals and help detoxify them [37, 38]. This ability to chelate metals may explain why Zn-Cys solution showed the least harmful effects to the *C. peltigerae.*

Subsequently, the UV protective effect of various concentrations of Zn, Cys, Zn-Cys complex, and Zn/Cys photoproducts was evaluated on *C. peltigerae* (Fig. 3). Microalgae were irradiated with UV-C light for 10 min and subsequently the growth cure was measured (see Sect. 2.3). Cys showed no significant UV protective effect (Fig. 3A). In case of zinc (Fig. 3B), the UV protective effect was minimal. But the 20% Zn solution variant showed significantly higher growth throughout the whole experiment compared to the control. On the other hand, the Zn–Cys complex (Fig. 3C) and Zn/Cys photoproducts (Fig. 3D) showed significant UV protective properties, in case of Zn–Cys solution, the effect was most prominent. All concentrations of Zn–Cys solution showed significantly higher growth in 24, 48, and 72 h compared to the control. Zn/Cys solution in concentration of 10 and 20% also showed similar results. Cysteine is a component of glutathione (a key antioxidant), which is essential for reducing oxidative stress. Zinc helps regulate antioxidant enzyme activities, such as superoxide dismutase (SOD) and glutathione peroxidase (GPx), which play crucial roles in scavenging harmful ROS [39]. It is plausible that UV irradiation induces the generation of reactive oxygen species (ROS), which subsequently interact with cysteine, potentially modifying its chemical structure and influencing its metal-binding capacity [40, 41].

Based on the experimental results, it is evident that the 20% concentration is the most effective in providing protection against UV-induced stress in *C. peltigerae,* (Fig. S1). This optimal concentration appears to strike a balance

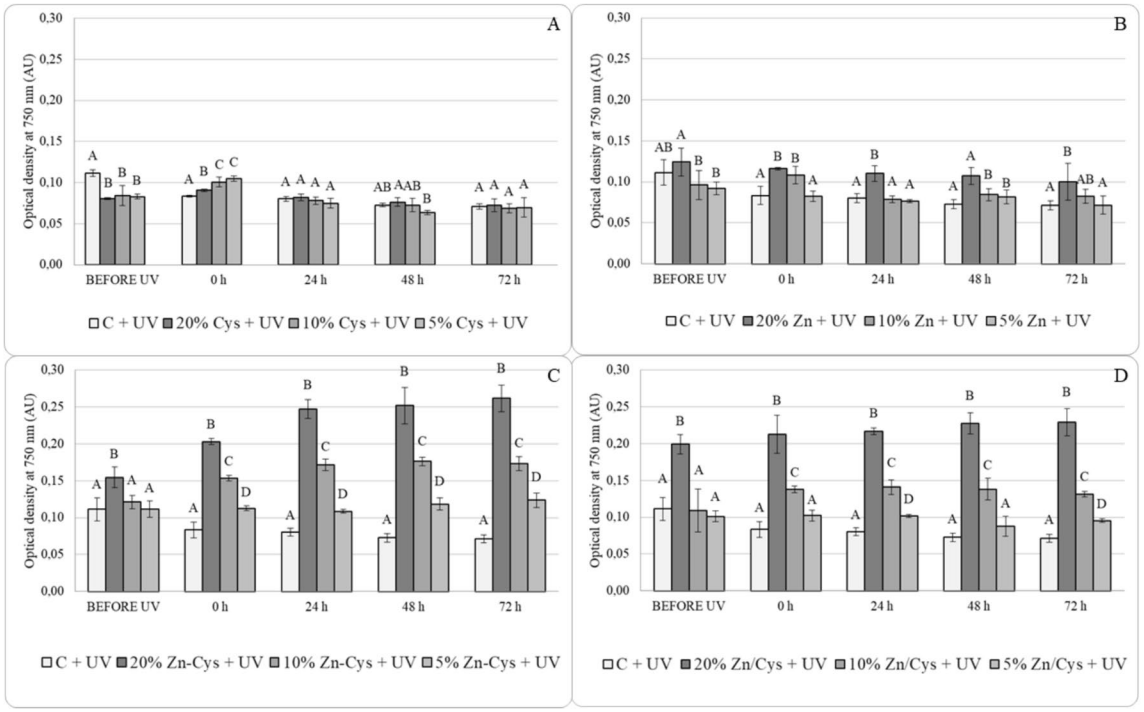

Fig. 3 Growth rate of *C. peltigerae* showing UV protective effect of 5, 10, and 20%: **A** cysteine, **B** zinc acetate, **C** Zn–Cys complex, and **D** Zn/Cys photoproducts. The Zn/Cys photoproduct treatment consisted of a Zn–Cys solution that had been pre-irradiated with UV-C light (254 nm) for 30 min outside of the biological system, prior to its application to algal cultures. The results are expressed as the mean ± standard error of the mean, and significant differences for various days are indicated by different capital letters in the graph (one-way ANOVA). We considered a value of p value < 0.05 to indicate a significant difference between groups, $n = 9$

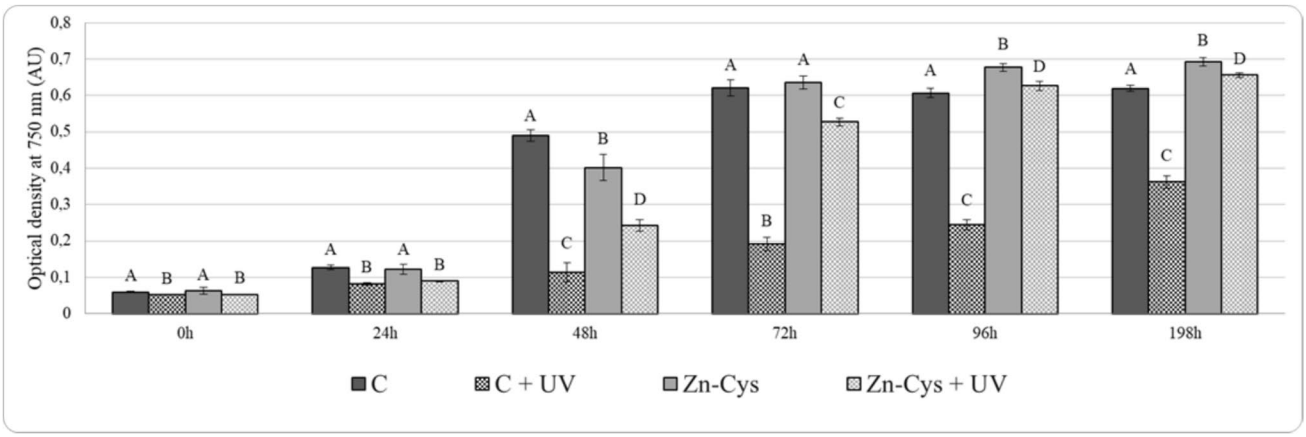

Fig. 4 Growth rate of *P. kessleri* showing UV protective effect of 20% Zn–Cys solution. The results are expressed as the mean ± standard error of the mean deviation, and significant differences for various days are indicated by different capital letters in the graph (one-way ANOVA). We considered a value of p value < 0.05 to indicate a significant difference between groups, $n = 9$

between toxic concentration, mitigating the harmful effects of UV irradiation, and supporting normal algal growth. Lower concentrations of the Zn-Cys solution, while still offering some degree of protection, were insufficient to fully counteract the detrimental impact of UV exposure.

3.3 UV protective properties of Zn-Cys using P. kessleri

After identifying the most effective UV-protective solution in previous experiments, the 20% Zn–Cys complex solution was subsequently tested on a different species of microalga to evaluate its efficacy (Fig. 4). *P. kessleri* was chosen specifically for its high tolerance and adaptability to stressors [22, 23]. The UV treatment (C + UV) consistently inhibits growth compared to the control, but to a lesser extent than in *C. peltigerae*, confirming *Parachlorella's* higher tolerance to UV light. The treatment with Zn–Cys solution initially slows growth but eventually supports a similar or even slightly enhanced growth compared to the control, showing the adaptability of *P. kessleri.* The irradiated treatment (Zn–Cys + UV) shows substantial negative effect initially, but over time, the treatment seems to promote algae growth similar to the non-irradiated variant. These results are consistent with our previous experiments with *C. peltigerae* showing the potential of Zn-Cys as UV protective agent.

3.4 Hyperspectral imaging demonstrated the protective effect of Zn-Cys against UV-induced damage using P. kessleri

For a further evaluation of UV protective effect of Zn–Cys solution, a robust method for monitoring the physiological state of microalgae cultures was used which involves the use of non-invasive hyperspectral imaging [42]. Hyperspectral imaging has been previously demonstrated to be a robust tool for identifying stress responses in various biological systems, such as cyanobacteria [43, 44], microalgae [45], or plants [46]. The impact of UV light on the composition and corresponding reflectance properties of algae was assessed under both control and UV-exposed conditions. Algae subjected to UV exposure exhibited increased reflectance in the red and blue visible spectral regions, indicating a reduced efficiency in light absorption by chlorophyll, Fig. 5A. The most pronounced alterations, however, were observed in the far-red region. Specifically, in the 700–800 nm range, the reflectance of UV-treated algae was significantly decreased, while an increase was noted between 950 and 1000 nm. The presence of Zn–Cys concurrently with UV exposure markedly mitigated the UV-induced changes in reflectance across the entire monitored spectral range. Notably,

Zn–Cys alone elicited a response in the algae similar to that of UV exposure, though the magnitude of this effect was substantially lower. Principal component analysis of the measured spectra revealed that UV light had the most significant influence on algae reflectance, whereas the application of Zn-Cys effectively nullified the UV-induced effects,

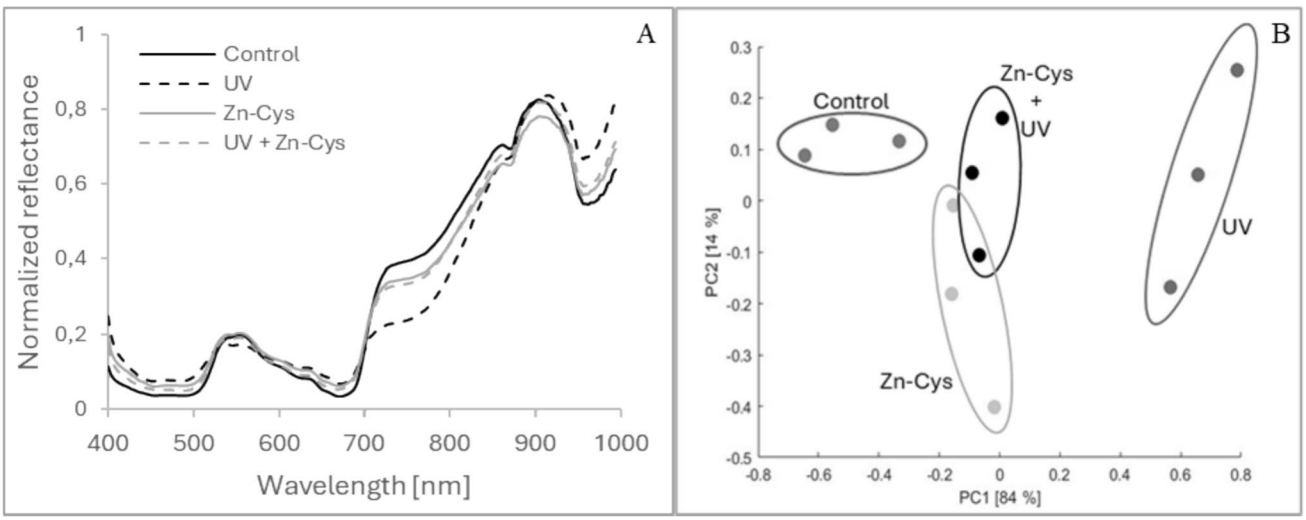

Fig. 5 Hyperspectral analysis of *P. kessleri* cultures. **A** Mean normalized reflectance spectra (3 independent cultivations) of the control and Zn-Cys-treated cultures (solid black and gray lines, respectively). Reflectance spectra of cultures exposed to UV light are shown with dashed lines (UV black dashed line, Zn–Cys + UV gray dashed line). **B** PCA based on hyperspectral reflectance data obtained from three independent cultivations. The resulting 2D plot captures over 98% of the total data variability, effectively visualizing the primary spectral variation among samples

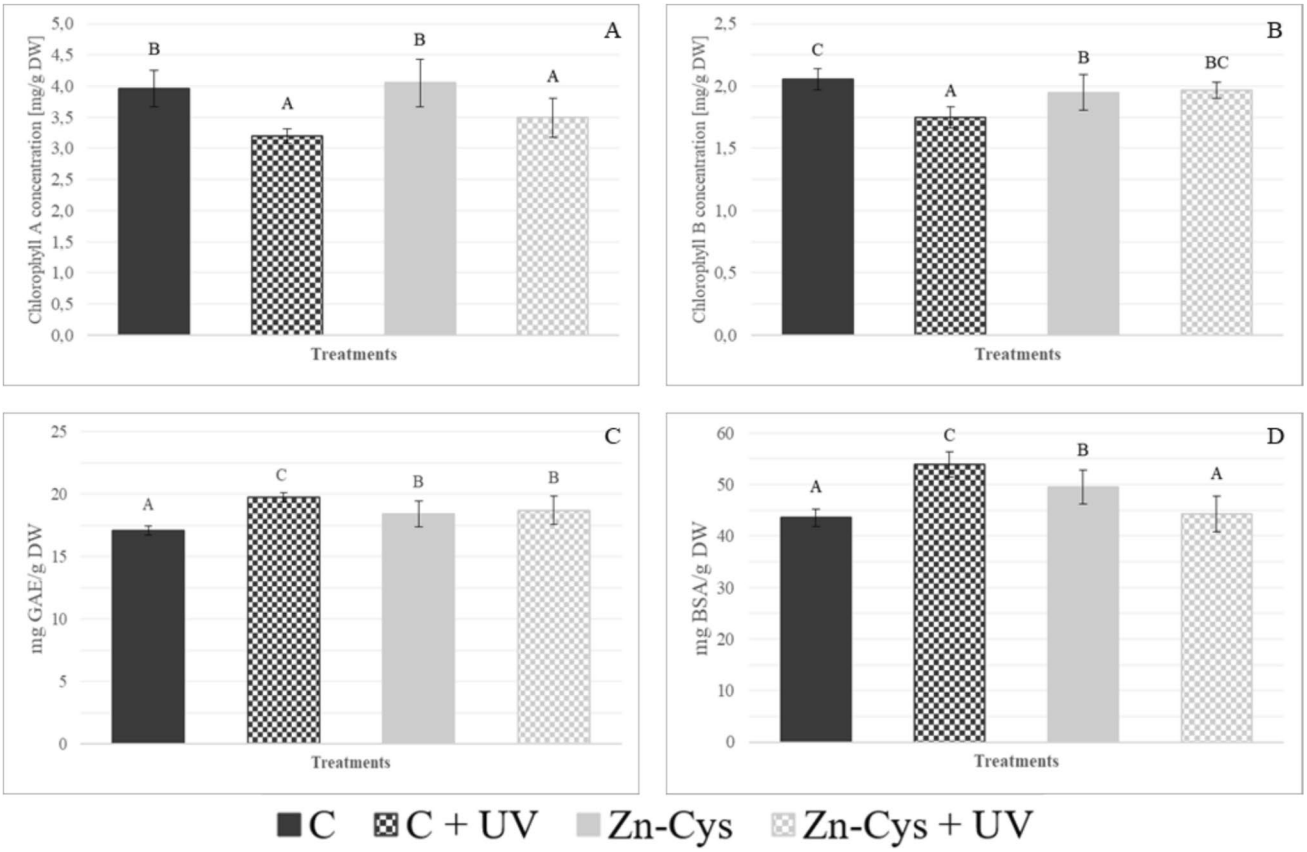

Fig. 6 Spectrophotometric analyses: **A** total chlorophyll A concentration, **B** total chlorophyll B concentration, **C** total polyphenol concentration, **D** total protein concentration. The results are expressed as the mean ± standard error of the mean deviation, and significant differences are indicated by different capital letters in the graph (one-way ANOVA). We considered a p value < 0.05 to indicate a significant difference between groups, $n = 9$

(Fig. 5B). The use of hyperspectral imaging in this study proved to be an effective method for detecting and analyzing physiological changes in microalgae. These results are consistent with the growth curve presented in Fig. 4 and provide evidence that the Zn-Cys treatment exhibits UV protective properties.

3.5 Spectrophotometric analyses of Z. mays

The protective effect of Zn-Cys was subsequently monitored in the agriculturally important crop maize (*Z. mays L.*), in in vitro conditions, Fig. 6. Spectrophotometric analyses of chlorophyll content showed a significantly higher concentration of chlorophyll B (Fig. 6B) in irradiated plants treated with Zn-Cys compared to irradiated control plants. With concentration of chlorophyll A (Fig. 6A), the difference between irradiated treated plants and irradiated control plants was not statistically significant. Even so, the concentration of chlorophyll A in irradiated control plants was lower. This finding aligns with literature, where zinc has been observed to play a role in stabilizing chlorophyll and preventing its degradation under stress conditions [47, 48]. Spectrophotometric analyses of total polyphenol content (Fig. 6C) confirm the previous results. The concentration of polyphenols in irradiated control plants was significantly higher than in irradiated plants treated with Zn–Cys, which indicates a higher level of oxidative stress, as polyphenols often accumulate as part of the plant's defense response [49, 50]. Other literature also affirms that the accumulation of phenolic compounds in response to UV radiation is a critical component of the plant's defense strategy. This response not only provides photoprotection but also mitigates the oxidative damage associated with UV stress [51, 52]. Lastly, the total protein content (Fig. 6D) also exhibited similar results. The concentration of proteins in irradiated control plants was significantly higher than in irradiated treated plants. Higher protein content may indicate higher production of defense proteins, therefore indicating more stress in irradiated control plants [53]. Literature also suggests that that exposure to UV radiation triggers a significant upregulation in the synthesis of a wide array of defense proteins in plants [54].

Another possible explanation is that plants may increase chloroplast protein synthesis as a compensatory response to maintain photosynthetic efficiency under stress. Studies have shown that UV-B exposure can stimulate chloroplast development and enhance the expression of chloroplast-associated proteins [55, 56]. Although direct evidence is limited, it is plausible that UV-C radiation may induce similar responses, prompting an increase in chloroplast protein synthesis as part of the plant's broader stress adaptation strategy.

Application of Zn–Cys exhibits a significant UV protective effect on both microalgae and plants. Zn–Cys probably prevents the formation of free radicals, mitigating the damaging effects of UV radiation by reducing oxidative stress and enhancing the stability of cellular structures. In plants and microalgae, Zn-Cys application may contribute to preserving chlorophyll content and promoting overall health.

4 Conclusion

In this study, we investigated the toxicity and UV protective properties of the zinc-cysteine complex (Zn–Cys), its precursors (Zn and Cys), and photoproducts (Zn/Cys). The Zn–Cys complex was synthesized from zinc acetate, L-cysteine, and phosphate buffer at pH 7. Fluorescence characterization confirmed the formation of Zn/Cys photoproducts, although further characterization is still required. Based on our initial experiments with *C. peltigerae*, we determined that a 20% Zn–Cys solution is the most effective in protecting cells from UV-induced damage. It did not negatively affect standard algal growth while providing the highest level of protection against UV irradiation. Lower concentrations offered some degree of UV protection but were insufficient to maintain standard algal growth. In contrast, zinc acetate or L-cysteine alone offered minimal UV protection and failed to support standard algal growth. The UV protective effect of the 20% Zn–Cys solution was also confirmed in experiments with *P. kessleri* and *Z. mays* L. This study highlights the potential of zinc and cysteine as protective agents against UV stress, with practical implications for enhancing resilience in agricultural systems and algae cultivation under challenging environmental conditions. However, further research should focus on the molecular and biochemical mechanisms underlying the protective effects observed in both microalgae and plants. In addition, a more comprehensive characterization of the Zn–Cys complexes and their Zn/Cys photoproducts formed under UV irradiation is necessary to assess their stability, efficacy, duration of the UV protective effect, and potential interactions with cellular components. This future work is critical for optimizing the application of Zn–Cys complexes in practical settings, ensuring their effectiveness in large-scale agricultural and biotechnological applications. Ultimately, expanding our understanding of these complexes could lead to the development of novel UV protection strategies that benefit a wide range of organisms, contributing to more sustainable and resilient agricultural practices and bioengineering solutions. The data that support the findings of this study are available from the corresponding author upon reasonable request.

Supplementary Information The online version contains supplementary material available at https://doi.org/10.1007/s43630-025-00740-9.

Acknowledgements The authors would like to express their gratitude to Mendel University in Brno for supporting this research through the IGA project (AF-IGA2023-IP-064)

Funding Open access publishing supported by the institutions participating in the CzechELib Transformative Agreement.

Data availability The data that support the findings of this study are available from the corresponding author upon reasonable request.We have added this sentence at the end of the Conclusion section.

Declarations

Conflict of interest Corresponding author Lukas Nejdl is the founder and scientific director of Lightly Technologies s.r.o., a company that utilizes light-driven reactions for forensic applications and food quality control. The authors declare that they have no known competing financial interests or personal relationships that could have influenced the work reported in this paper.

References

1. Li, J. G., Zhang, D., Guo, Z. Y., Chen, Z. H., Jiang, X., Larson, J. M., et al. (2024). Light-driven C-H activation mediated by 2D transition metal dichalcogenides. *Nature Communications*. https://doi.org/10.1038/s41467-024-49783-z. PubMed PMID: WOS:001261751100017.
2. Li, Y. L., Gao, Y. X., Deng, Z. J., Cao, Y. T., Wang, T., Wang, Y., et al. (2023). Visible-light-driven reversible shuttle vicinal dihalogenation using lead halide perovskite quantum dot catalysts. *Nature Communications*. https://doi.org/10.1038/s41467-023-40359-x. PubMed PMID: WOS:001040308300001.
3. Czyz, M. L., Horngren, T. H., Kondopoulos, A. J., Franov, L. J., Forni, J. A., Pham, L., et al. (2024). Photocatalytic generation of alkyl carbanions from aryl alkenes. *Nature Catalysis*.

https://doi.org/10.1038/s41929-024-01237-x. PubMedPMID: WOS:001339321900001.
4. Hoyle, C. E., & Bowman, C. N. (2010). Thiol-ene click chemistry. *Angew Chem-Int Edit, 49*(9), 1540–1573. https://doi.org/10.1002/anie.200903924. PubMedPMID:WOS:000275234800004.
5. Nejdl, L., Petera, L., Sponer, J., Zemánková, K., Pavelicová, K., Knízek, A., et al. (2022). Quantum dots in peroxidase-like chemistry and formamide-based hot spring synthesis of nucleobases. *Astrobiology, 22*(5), 541–551. https://doi.org/10.1089/ast.2021.0099. PubMedPMID:WOS:000776448100001.
6. Nejdl, L., Zemankova, K., Havlikova, M., Buresova, M., Hynek, D., Xhaxhiu, K., et al. (2020). UV-induced nanoparticles-formation, properties and their potential role in origin of life. *Nanomaterials*. https://doi.org/10.3390/nano10081529. PMID: WOS:000564810900001.
7. Fialova, T., Vaculovicova, M., Stefanik, M., Mravec, F., Buresova, M., Vodova, M., et al. (2024). Light-triggered reactions in a new "light" of nanoparticles engineering. *Journal of Photochemistry and Photobiology a-Chemistry*. https://doi.org/10.1016/j.jphotochem.2024.115667. PubMed PMID: WOS:001232262400001.
8. Vanhaelewyn, L., Van Der Straeten, D., De Coninck, B., & Vandenbussche, F. (2020). Ultraviolet radiation from a plant perspective: The Plant-microorganism context. *Frontiers in Plant Science*. https://doi.org/10.3389/fpls.2020.597642. PMID: WOS:000603030600001.
9. Llorens, L., Neugart, S., Vandenbussche, F., & Castagna, A. (2020). Editorial: ultraviolet radiation: friend or foe for plants? *Frontiers in Plant Science*. https://doi.org/10.3389/fpls.2020.00541. PubMed PMID: WOS:000535555000001.
10. Keaney, D., Lucey, B., & Finn, K. (2024). A Review of environmental challenges facing martian colonisation and the potential for terrestrial microbes to transform a toxic extraterrestrial environment. *Challenges., 15*(1), 5. https://doi.org/10.3390/challe15010005
11. Pace, N. J., & Weerapana, E. (2014). Zinc-binding cysteines: diverse functions and structural motifs. *Biomolecules, 4*(2), 419–434. https://doi.org/10.3390/biom4020419. PubMedPMID :WOS:000215154100004.
12. Dmytryk, A., & Chojnacka, K. (2018). Algae as fertilizers, biostimulants, and regulators of plant growth. In K. Chojnacka, P. P. Wieczorek, G. Schroeder, & I. Michalak (Eds.), *Algae biomass: characteristics and applications: Towards algae-based products* (pp. 115–122). Springer International Publishing.
13. Ammar, E. E., Aioub, A. A. A., Elesawy, A. E., Karkour, A. M., Mouhamed, M. S., Amer, A. A., et al. (2022). Algae as bio-fertilizers: Between current situation and future prospective. *Saudi Journal of Biological Sciences, 29*(5), 3083–3096. https://doi.org/10.1016/j.sjbs.2022.03.020
14. Roque, J., Brito, Â., Rocha, M., Pissarra, J., Nunes, T., Bessa, M., et al. (2023). Isolation and characterization of soil cyanobacteria and microalgae and evaluation of their potential as plant biostimulants. *Plant and Soil, 493*(1), 115–136. https://doi.org/10.1007/s11104-023-06217-x
15. Baweja, P., Kumar, S., & Kumar, G. (2019). Organic Fertilizer from Algae: A Novel Approach Towards Sustainable Agriculture. In B. Giri, R. Prasad, Q.-S. Wu, & A. Varma (Eds.), *Biofertilizers for sustainable agriculture and environment* (pp. 353–370). Springer International Publishing.
16. Udayan, A., Pandey, A. K., Sharma, P., Sreekumar, N., & Kumar, S. (2021). Emerging industrial applications of microalgae: Challenges and future perspectives. *Systems Microbiology and Biomanufacturing., 1*(4), 411–431. https://doi.org/10.1007/s43393-021-00038-8
17. Blaise, C., Férard, J.-F., & Vasseur, P. (2018). Microplate toxicity tests with microalgae: A review. *Microscale testing in aquatic toxicology* (pp. 269–88). OAPEN Library.
18. Nyholm, N., & Källqvist, T. (1989). Methods for growth inhibition toxicity tests with freshwater algae. *Environmental Toxicology and Chemistry, 8*(8), 689–703. https://doi.org/10.1002/etc.5620080807
19. Gardia-Parège, C., Kim Tiam, S., Budzinski, H., Mazzella, N., Devier, M.-H., & Morin, S. (2022). Pesticide toxicity towards microalgae increases with environmental mixture complexity. *Environmental Science and Pollution Research, 29*(20), 29368–29381. https://doi.org/10.1007/s11356-021-17811-w
20. Elpiniki, S., Alexandra, S., Georgios, C., & Nicholaos, D. (2019). Maize as energy crop. In H. Akbar (Ed.), *Maize* (p. 1). IntechOpen.
21. Trout, T. J., & DeJonge, K. C. (2017). Water productivity of maize in the US high plains. *Irrigation Science, 35*(3), 251–266. https://doi.org/10.1007/s00271-017-0540-1
22. Liu, X., Zhao, J., Feng, J., Lv, J., Liu, Q., Nan, F., et al. (2022). A Parachlorella kessleri (Trebouxiophyceae, Chlorophyta) strain tolerant to high concentration of calcium chloride. *Journal of Eukaryotic Microbiology., 69*(1), Article e12872. https://doi.org/10.1111/jeu.12872
23. Rathod, J. P., Prakash, G., Vira, C., & Lali, A. M. (2016). Trehalose phosphate synthase overexpression in Parachlorella kessleri improves growth and photosynthetic performance under high light conditions. *Preparative Biochemistry & Biotechnology., 46*(8), 803–809. https://doi.org/10.1080/10826068.2015.1135465
24. Nguyen, C., Sagan, V., Maimaitiyiming, M., Maimaitijiang, M., Bhadra, S., & Kwasniewski, M. T. (2021). Early detection of plant viral disease using hyperspectral imaging and deep learning. *Sensors., 21*(3), 742.
25. Lichtenthaler, H., & Wellburn, A. R. (1985). Determination of total carotenoids and chlorophylls a and b of leaf in different solvents. *Biochemical Society Transactions, 11*, 591–592.
26. Koşar, M., Dorman, H. J. D., & Hiltunen, R. (2005). Effect of an acid treatment on the phytochemical and antioxidant charateristics of extracts from selected Lamiaceae species. *Food Chemistry, 91*, 525–533. https://doi.org/10.1016/j.foodchem.2004.06.029
27. Bradford, M. M. (1976). A rapid and sensitive method for the quantitation of microgram quantities of protein utilizing the principle of protein-dye binding. *Analytical Biochemistry, 72*, 248–254. https://doi.org/10.1006/abio.1976.9999. PubMed PMID: 942051.
28. Foley, S., & Enescu, M. (2007). A Raman spectroscopy and theoretical study of zinc-cysteine complexation. *Vibrational Spectroscopy., 44*(2), 256–265. https://doi.org/10.1016/j.vibspec.2006.12.004. PubMedPMID:WOS:000248604400008.
29. Brandt, E. G., Hellgren, M., Brinck, T., Bergman, T., & Edholm, O. (2009). Molecular dynamics study of zinc binding to cysteines in a peptide mimic of the alcohol dehydrogenase structural zinc site. *Physical Chemistry Chemical Physics, 11*(6), 975–983. https://doi.org/10.1039/b815482a.PubMedPMID:WOS:000262850600011
30. Nejdl, L., Zitka, J., Mravec, F., Milosavljevic, V., Zitka, O., Kopel, P., et al. (2017). Real-time monitoring of the UV-induced formation of quantum dots on a milliliter, microliter, and nanoliter scale. *Microchimica Acta, 184*(5), 1489–1497. https://doi.org/10.1007/s00604-017-2149-8. PubMedPMID:WOS:000399900600025.
31. Croce, A. C. (2021). Light and Autofluorescence Multitasking Features in Living Organisms. *Photochem, 1*(2), 67–124. https://doi.org/10.3390/photochem1020007. PubMedPMID: WOS:001268588500001.
32. Nicolaï, M. P. J., Bok, M. J., Abalos, J., D'Alba, L., Shawkey, M. D., & Goldenberg, J. (2024). The function and consequences of fluorescence in tetrapods. *Proceedings of the National Academy of Sciences., 121*(24), Article e2318189121. https://doi.org/10.1073/pnas.2318189121

33. Suma, H. R., Prakash, S., & Eswarappa, S. M. (2020). Naturally occurring fluorescence protects the eutardigrade Paramacrobiotus sp. From ultraviolet radiation: UV tolerance by fluorescence. *Biology Letters*. https://doi.org/10.1098/rsbl.2020.0391
34. Aravantinou, A. F., Tsarpali, V., Dailianis, S., & Manariotis, I. D. (2015). Effect of cultivation media on the toxicity of ZnO nanoparticles to freshwater and marine microalgae. *Ecotoxicology and Environmental Safety, 114*, 109–116. https://doi.org/10.1016/j.ecoenv.2015.01.016
35. Samei, M., Sarrafzadeh, M.-H., & Faramarzi, M. A. (2019). The impact of morphology and size of zinc oxide nanoparticles on its toxicity to the freshwater microalga, Raphidocelis subcapitata. *Environmental Science and Pollution Research., 26*(3), 2409–2420. https://doi.org/10.1007/s11356-018-3787-z
36. Vingiani, G. M., Gasulla, F., Barón-Sola, Á., Sobrino-Plata, J., Henández, L. E., & Casano, L. M. (2021). Physiological and molecular alterations of phycobionts of genus trebouxia and coccomyxa exposed to cadmium. *Microbial Ecology, 82*(2), 334–343. https://doi.org/10.1007/s00248-021-01685-z
37. Huang, Z., Zeng, Z., Chen, A., Zeng, G., Xiao, R., Xu, P., et al. (2018). Differential behaviors of silver nanoparticles and silver ions towards cysteine: Bioremediation and toxicity to Phanerochaete chrysosporium. *Chemosphere, 203*, 199–208. https://doi.org/10.1016/j.chemosphere.2018.03.144
38. Mera, R., Torres, E., & Abalde, J. (2014). Sulphate, more than a nutrient, protects the microalga Chlamydomonas moewusii from cadmium toxicity. *Aquatic Toxicology., 148*, 92–103. https://doi.org/10.1016/j.aquatox.2013.12.034
39. Li, X., Yang, C., Zeng, G., Wu, S., Lin, Y., Zhou, Q., et al. (2020). Nutrient removal from swine wastewater with growing microalgae at various zinc concentrations. *Algal Research, 46*, Article 101804. https://doi.org/10.1016/j.algal.2020.101804
40. Winterbourn, C. C., & Hampton, M. B. (2008). Thiol chemistry and specificity in redox signaling. *Free Radical Biology and Medicine, 45*(5), 549–61. https://doi.org/10.1016/j.freeradbiomed.2008.05.004. Epub 20080516 PubMed PMID: 18544350.
41. Schöneich, C. (2008). Mechanisms of protein damage induced by cysteine thiyl radical formation. *Chemical Research in Toxicology, 21*(6), 1175–9. https://doi.org/10.1021/tx800005u. Epub 20080325 PubMed PMID: 18361510.
42. Pääkkönen, S., Pölönen, I., Raita-Hakola, A.-M., Carneiro, M., Cardoso, H., Mauricio, D., et al. (2024). Non-invasive monitoring of microalgae cultivations using hyperspectral imager. *Journal of Applied Phycology., 36*(4), 1653–1665. https://doi.org/10.1007/s10811-024-03256-4
43. Deng, T., DePaoli, D., Bégin, L., Jia, N., Torres de Oliveira, L., Côté, D. C., et al. (2021). Versatile microfluidic platform for automated live-cell hyperspectral imaging applied to cold climate cyanobacterial biofilms. *Analytical Chemistry, 93*(25), 8764–73. https://doi.org/10.1021/acs.analchem.0c05446
44. Pokrzywinski KL, Morgan C, Bourne SG, Reif MK, Matheson KB, Hammond SL. (2021). A novel laboratory method for the detection and identification of cyanobacteria using hyperspectral imaging: hyperspectral imaging for cyanobacteria detection
45. Salmi, P., Eskelinen, M. A., Leppänen, M. T., & Pölönen, I. (2021). Rapid quantification of microalgae growth with hyperspectral camera and vegetation indices. *Plants., 10*(2), 341.
46. Williams, D., Karley, A., Britten, A., McCallum, S., & Graham, J. (2023). Raspberry plant stress detection using hyperspectral imaging. *Plant Direct, 7*(3), Article e490. https://doi.org/10.1002/pld3.490
47. Rajput, V. D., Minkina, T., Fedorenko, A., Chernikova, N., Hassan, T., Mandzhieva, S., et al. (2021). Effects of zinc oxide nanoparticles on physiological and anatomical indices in spring barley tissues. *Nanomaterials, 11*(7), 1722.
48. Cherif, J., Derbel, N., Nakkach, M., Hv, B., Jemal, F., & Lakhdar, Z. B. (2010). Analysis of in vivo chlorophyll fluorescence spectra to monitor physiological state of tomato plants growing under zinc stress. *Journal of Photochemistry and Photobiology B: Biology, 101*(3), 332–9. https://doi.org/10.1016/j.jphotobiol.2010.08.005
49. Chen, Y., Huang, L., Liang, X., Dai, P., Zhang, Y., Li, B., et al. (2020). Enhancement of polyphenolic metabolism as an adaptive response of lettuce (Lactuca sativa) roots to aluminum stress. *Environmental Pollution., 261*, Article 114230. https://doi.org/10.1016/j.envpol.2020.114230
50. Sharma, A., Shahzad, B., Rehman, A., Bhardwaj, R., Landi, M., & Zheng, B. (2019). Response of phenylpropanoid pathway and the role of polyphenols in plants under abiotic stress. *Molecules, 24*(13), 2452.
51. Höll, J., Lindner, S., Walter, H., Joshi, D., Poschet, G., Pfleger, S., et al. (2019). Impact of pulsed UV-B stress exposure on plant performance: How recovery periods stimulate secondary metabolism while reducing adaptive growth attenuation. *Plant, Cell & Environment., 42*(3), 801–814. https://doi.org/10.1111/pce.13409
52. Rodríguez-Calzada, T., Qian, M., Strid, Å., Neugart, S., Schreiner, M., Torres-Pacheco, I., et al. (2019). Effect of UV-B radiation on morphology, phenolic compound production, gene expression, and subsequent drought stress responses in chili pepper (Capsicum annuum L.). *Plant Physiology and Biochemistry., 134*, 94–102. https://doi.org/10.1016/j.plaphy.2018.06.025
53. Przymusiński, R., Rucińska, R., & Gwóźdź, E. A. (2004). Increased accumulation of pathogenesis-related proteins in response of lupine roots to various abiotic stresses. *Environmental and Experimental Botany, 52*(1), 53–61. https://doi.org/10.1016/j.envexpbot.2004.01.006
54. Du, H., Liang, Y., Pei, K., & Ma, K. (2011). UV radiation-responsive proteins in rice leaves: a proteomic analysis. *Plant and Cell Physiology, 52*(2), 306–316. https://doi.org/10.1093/pcp/pcq186
55. Li, H., Li, Y., Deng, H., Sun, X., Wang, A., Tang, X., et al. (2018). Tomato UV-B receptor SlUVR8 mediates plant acclimation to UV-B radiation and enhances fruit chloroplast development via regulating SlGLK2. *Scientific Reports, 8*(1), 6097. https://doi.org/10.1038/s41598-018-24309-y
56. Gao, L., Wang, X., Li, Y., & Han, R. (2019). Chloroplast proteomic analysis of Triticum aestivum L seedlings responses to low levels of UV-B stress reveals novel molecular mechanism associated with UV-B tolerance. *Environmental Science and Pollution Research, 26*(7), 7143–55. https://doi.org/10.1007/s11356-019-04168-4